

Spectral analysis by a video camera in a holographic optical tweezers setup

SŁAWOMIR DROBCZYŃSKI^{1*}, KAMILA DUŚ-SZACHNIEWICZ²,
KRZYSZTOF SYMONOWICZ², DARIA GŁOGOCKA³

¹Institute of Physics, Wrocław University of Technology,
Wybrzeże Wyspiańskiego 27, 50-370 Wrocław, Poland

²Department of Pathology, Faculty of Medicine, Wrocław Medical University,
Marcinkowskiego 1, 50-368 Wrocław, Poland

³Laboratory for Biophysics of Lipid Aggregates,
Institute of Biomedical Engineering and Instrumentation,
Wrocław University of Technology, pl. Grunwaldzki 13, 50-377 Wrocław, Poland

*Corresponding author: slawomir.drobczynski@pwr.edu.pl

We discuss the basic parameters of the holographic tweezers equipped with a diode laser and cheap video camera. We compare these parameters with the system using a fast camera and high power Nd:YAG laser. The measured parameters are: the power spectra density calculated from tracing the position of the micron polystyrene beads and the trap stiffness. We show that this cheap optical tweezers system is sufficient for experiments in microbiology.

Keywords: holographic optical tweezers, power spectrum density, video analysis.

1. Introduction

Optical tweezers enable micro objects capturing and moving. The forces and displacements can be also measured with pN and nm resolution, respectively [1]. To measure the forces acting on trapped micro objects, the optical trap stiffness k_h [2, 3] must be known in prior. For optical trap stiffness determination, the model objects like polystyrene beads having size 1–5 μm are commonly used. The trapped beads oscillate around an equilibrium point due to thermal effects. These oscillations are precisely measured and their power spectra density (PSD) is computed. Then the Lorentzian function is fitted to the PSD, which provides information about a corner frequency f_c . The corner frequency is the frequency where the power of the thermal motion has

dropped to the half of its asymptotic value. The parameter f_c is proportional to the trap stiffness k_h [4]

$$k_h = 12\pi^2 f_c \eta R_B \quad (1)$$

where η is the fluid viscosity and R_B is the beads radius.

A commonly used detector, in single trap optical tweezers, is a quadrant photodiode (QPD) [5]. The QPD allows the sampling frequency of 10 kHz, which is sufficient for most demanding optical trap stiffness measurements. The trap stiffness measured in optical tweezers (equipped with Nd:YAG laser) is typically at the range from 10^{-5} to 10^{-4} N/m, which corresponds to f_c value from 100 Hz to 1 kHz.

To expand the optical tweezers potential, the holographic technique was adopted for optical trap creation [6]. The holographic optical tweezers enable the generation of few tens of traps simultaneously. The position of each trap can be controlled in x - y - z axis independently. Also different kinds of traps (light, dark [7], Bessel [8]) can be generated simultaneously. In the holographic optical tweezers, the traps are generated by writing series of appropriate holograms on the spatial light modulator (SLM). The holograms are reconstructed at the focused plane of the high NA objective (Fig. 1).

Measuring the trap stiffness in a multi-trap mode with QPD is a difficult task. It is hard to separate the influence of different traps on the signal captured by the QPD. To avoid these problems, the holographic optical tweezers are equipped with a fast video camera (more than 5000 frames per second; fps). The fast video camera enables

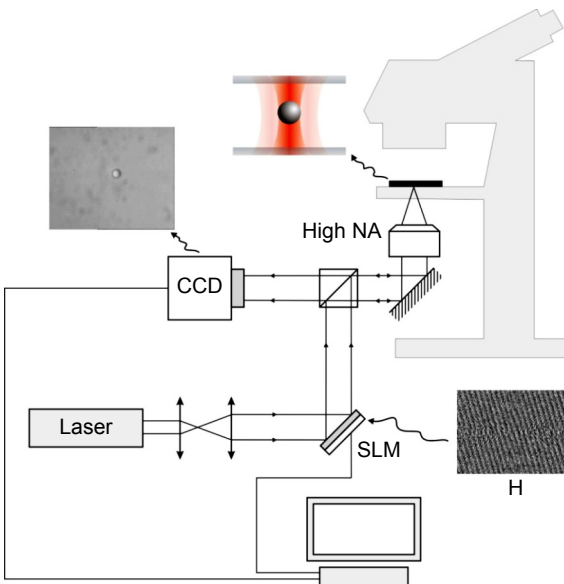


Fig. 1. Scheme of the holographic optical tweezers based on the reverse biological microscope.

tracking the number of traps simultaneously. In [9] a comparative analysis of both detectors, QPD and high speed camera in the holographic optical tweezers system is presented.

In this work we present a test of a cheap version of the holographic optical tweezers. To lower the costs, the laser diode was used together with an inexpensive video camera. The laser diode power is relatively small (when compared with Nd:YAG laser) and the trap stiffness is relatively low. However, it is still sufficient for many experiments including trapping and moving the living cells. On the other hand, the relatively small trap stiffness results in a smaller corner frequency f_c in the signal spectrum. In our system, the trap stiffness was about $k_h = 10^{-6}$ N/m and the sampling frequency might be below 1 kHz. By reducing the registration area ROI (region of interest) on the camera image sensor, we achieved a speed up to 2000 fps. With our software, a single camera can be used for various tasks: imaging the sample, data analysis and traps position control. To make the system friendly for the user who has no technical experience, the microscopic objects are controlled via a touch screen. The user touches the trap image displayed on the screen and moves it just by moving the finger to the desired position. The holographic tweezers with a standard video camera and a diode laser are cheaper and can be made more compact.

2. Video analysis

In the motion detection system, which is based on the QPD, the trapped object displacement is proportional to the output voltage of the photosensitive element. When using the video camera, the image processing procedures must be applied to measure the trapped object position. These procedures must be fast enough to precede a large collection of frames in an acceptable time. The PSD measurements performed with a standard camera were compared with measurements performed with a high speed camera MC1362 (Mikrotron GmbH), CameraLink, CMOS sensor, 1280×1024. This camera can record up to 10 000 fps in the region of 150×160 pixels. Optical traps were generated with a pigtail single mode diode laser $\lambda = 980$ nm having a maximum output power of 450 mW. The sequence of 40 000 frames at $f_s = 5 000$ fps and exposure time 150 ms was recorded. With such a fast shutter speed, the bright light source for image illumination must be used. In order to avoid additional sample heating, we used high-power white LEDs. Image analysis was performed with the help of a home written (in C++) computer program. In order to speed up the calculations, the numerical procedures optimized for Intel IPP library computing (Intel® Integrated Performance Primitives) were applied. Two algorithms for the polystyrene beads position were tested. In the first, the position of beads mass center (x_0, y_0) was calculated with the following equations:

$$x_0 = \frac{\sum_j \sum_k x_k P_{j,k}}{\sum_j \sum_k P_{j,k}} \quad (2)$$

$$y_0 = \frac{\sum_j \sum_k y_j P_{j,k}}{\sum_j \sum_k P_{j,k}} \quad (3)$$

where: j is the row, k is the column, x, y are the positions in pixels, P is the pixel brightness.

In the second algorithm, the coordinates of a center of the circle written into the object were calculated. For this purpose, the Kasa method (non-iterative) [10] for finding the center of the circle with the radius R defined by i -points was used (x_i, y_i)

$$F(a, b, R) = \sum_i \left[(x_i - a)^2 + (y_i - b)^2 - R^2 \right]^2 \quad (4)$$

To describe a circle on the beads, its image (Fig. 2a) contrast was reversed (Fig. 2b) and binarized (Fig. 2c). Figure 2d shows an example of a circle inscribed in the image of the trapped beads.

Figures 3 and 4 show the Lorentzian fitted to the data obtained by: calculating the center of mass of the beads in the optical trap and the Kasa method. The figures

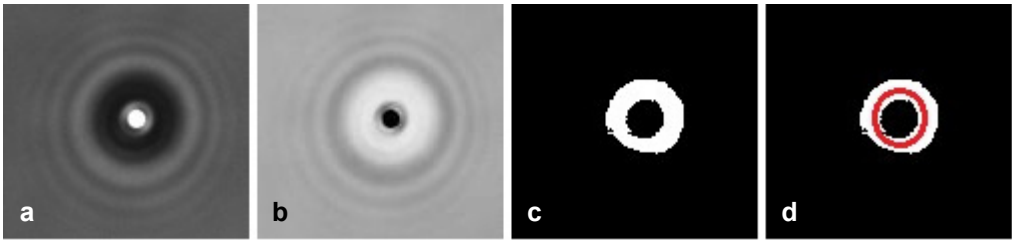


Fig. 2. Image of 3 μm polystyrene bead (Polybead[®] Polystyrene Microsphere) – a. Negative – b, binary – c, and circle fit – d.

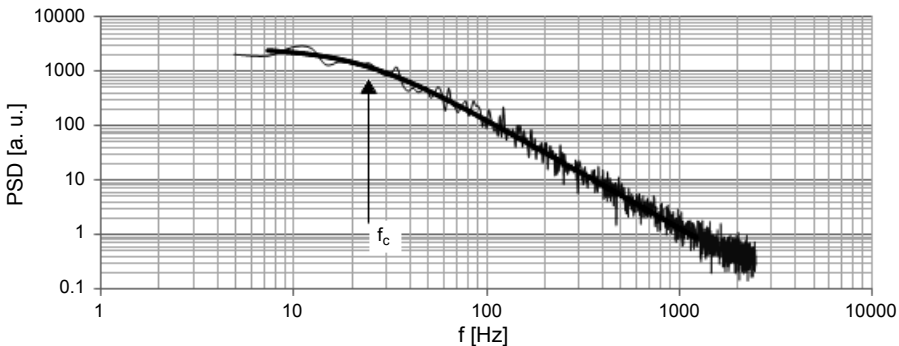


Fig. 3. The Lorentzian curve fitted to the data measured with a camera MC1362. The beads positions were found with the center of mass method. The camera speed was $f_s = 5000$ fps, $f_c = 25.1$ Hz, $k_h = 4.48 \times 10^{-6}$ N/m, $\sigma_{\text{trap}} = 15$ nm, $\sigma_{\text{fixed}} = 0.9$ nm.

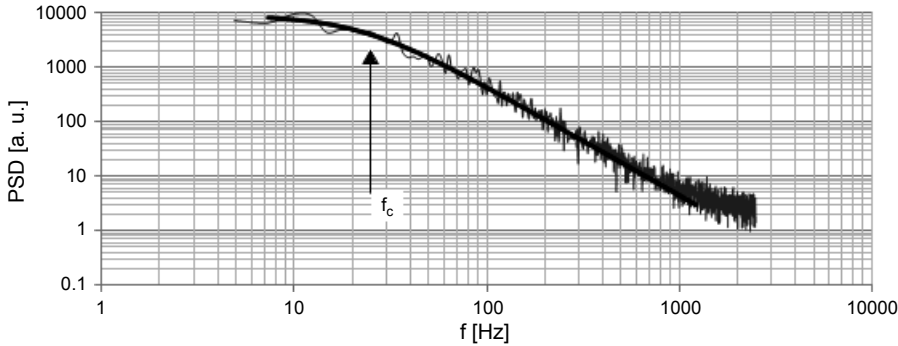


Fig. 4. The Lorentzian curve fitted to the data measured with a camera MC1362. The beads positions were found with the Kasa method. The camera speed was $f_s = 5000$ fps, $f_c = 25.1$ Hz, $k_h = 4.48 \times 10^{-6}$ N/m, $\sigma_{\text{trap}} = 16$ nm, $\sigma_{\text{fixed}} = 1$ nm.

were plotted for the same video sequence. Both procedures result in the same optical trap stiffness value.

The standard deviation σ was measured in two cases. In the first case σ_{fixed} , the beads were fixed to the microscope slide (no trapping forces were applied); while in the second case σ_{trap} , the beads in the optical trap were measured (these beads have no contact with the slide surface). The σ_{fixed} depends on the system mechanical stability and electronic noise. By comparing these both values of standard deviation, the system stability can be evaluated [11]. In general, the σ_{fixed} must be much smaller than σ_{trap} ; otherwise the results are too much blurred by noise. In our case, the standard deviation σ_{fixed} was typically about 20 times smaller than σ_{trap} , which means that our measurements are reliable.

3. Results

Figure 5 shows an example of the typical Lorentzian obtained by GE680 camera (Allied Vision Technologies) Gigabit Ethernet interface, 1/3" CCD sensor, 640×480 for the ROI of 16×16 pixels and exposure time 150 μ s. The achieved write speed video sequences $f_s = 2000$ fps.

Figure 6 shows an example of the typical Lorentzian obtained by the camera UI-1540LE (IDS Imaging Development Systems GmbH) USB 2.0, 1/2" CMOS sensor, 1280×1024, for the ROI of 34×34 pixels and exposure time 150 μ s. The achieved write speed video sequences $f_s = 900$ fps. This was the highest fps we were able to drive this camera.

The experiments show that the cameras used in our experiments were sufficient for measuring the thermal motion of the trapped particles. The Lorentzian and the measured parameters were practically the same for both cameras and for the fast camera typically used for this purpose. Since the cameras were typical, we may expect that most of cameras available on the market can be used with holographic optical tweezers.

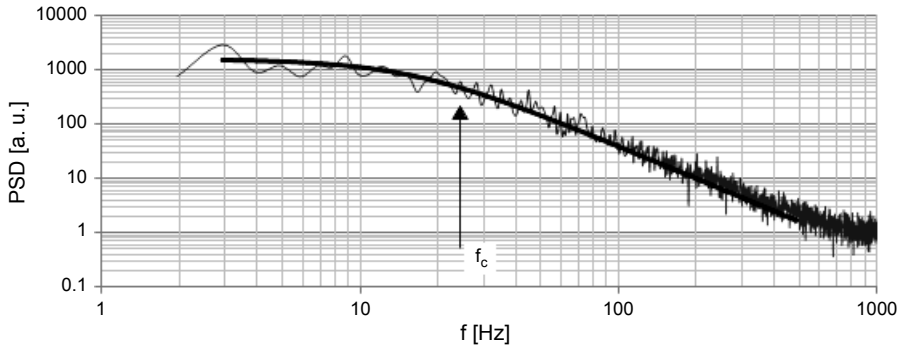


Fig. 5. The Lorentzian curve fitted to the data measured with a camera GE680. The beads positions were found with the center of mass method. The camera speed was $f_s = 2000$ fps, $f_c = 25.5$ Hz, $k_h = 4.55 \times 10^{-6}$ N/m, $\sigma_{\text{trap}} = 16$ nm, $\sigma_{\text{fixed}} = 0.9$ nm.

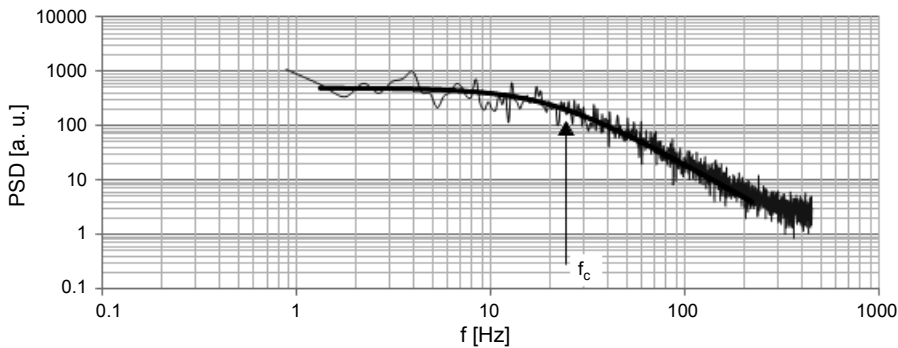


Fig. 6. The Lorentzian curve fitted to the data measured with a camera UI-1540LE. The beads positions were found with the center of mass method. The camera speed was $f_s = 900$ fps, $f_c = 25.7$ Hz, $k_h = 4.59 \times 10^{-6}$ N/m, $\sigma_{\text{trap}} = 15$ nm, $\sigma_{\text{fixed}} = 0.8$ nm.

The condition is to apply the special software to make the camera speed about 1 000 fps at the limited ROI. The trap stiffness cannot be also too high to keep the corner frequency f_c low enough.

Figure 7 shows an example of experiments with a cancer cell SW 620 squeezed by beads. Two polystyrene beads with a diameter of 3 μm were trapped and kept in place just behind the cell. The third trapped bead of the same size was used to push the cell membrane. Knowing static stiffness of the trap and measuring the displacement of the third bead, one can determine the strength of the cell membrane. Unfortunately, the stiffness of the unmodified cell membrane was too high to be measured in this way. The additional chemical cell modification was necessary for quantitative measurements. Nevertheless, the trap stiffness was large enough for cell capturing and positioning within the sample volume.

In the second example, the frequency analysis of the trapped beads motion was used to determine the viscosity of the liquid. At first, we determine the optical trap stiffness in the case of fluid of known viscosity η_1 and the beads of the radius R_B .

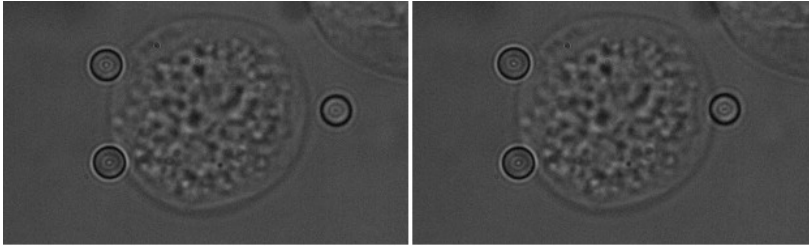


Fig. 7. Colorectal adenocarcinoma, human colon cancer SW620 cell line.

Without changing the laser power, the signal from the beads in the liquid of unknown viscosity η_x was recorded. After spectral analysis, the new value corner frequency f_{cx} was determined using the transformed Eq. (1)

$$\eta_x = \frac{k_h}{12\pi^2 f_{cx} R_B} \quad (5)$$

Figure 8 shows exemplary results.

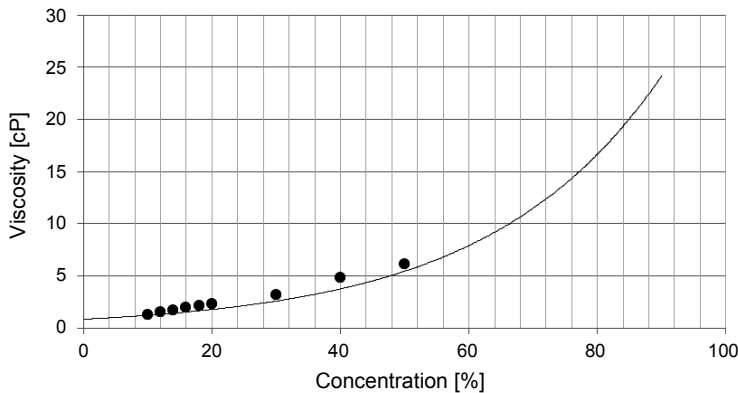


Fig. 8. The measured viscosity as a function of concentration (black dots). The solid line represents the data taken from physical tables.

With the optical tweezers, the viscosity can be measured locally, so its variation across the sample area can be mapped; for example, in the solution with the gradient of substance concentration.

4. Conclusions

We tested the holographic optical tweezers equipped with the cheap standard camera and laser diode. Due to the power limit, the experiments were limited to three traps generated simultaneously. The trap stiffness was about 5×10^{-6} N/m. On the other hand, small trap stiffness allows for measuring with standard video cameras provided they

are speeded up to 1000 fps. Many cameras can work with this speed, but the registration area must be limited. The necessary procedures for fast video stream processing and analysis were developed and successfully tested. The measured trap stiffness was in agreement with measurements performed with a high speed, low noise professional camera. The system was also successfully used for measuring the forces acting on the polystyrene bead, for cell manipulation and viscosity measurements.

Acknowledgements – This work was supported by the Polish Ministry of Scientific Research and Information Technology under Grant No. N N518 498839.

References

- [1] STEVENSON D., GUNN-MOORE F., DHOLAKIA K., *Light forces the pace: optical manipulation for biophotonics*, Journal of Biomedical Optics **15**(4), 2010, article 041503.
- [2] FARRÉ A., VAN DER HORST A., BLAB G.A., DOWNING B.P.B., FORDE N.R., *Stretching single DNA molecules to demonstrate high-force capabilities of holographic optical tweezers*, Journal of Biophotonics **3**(4), 2010, pp. 224–233.
- [3] SINGER W., BERNET S., HECKER N., RITSCH-MARTE M., *Three-dimensional force calibration of optical tweezers*, Journal of Modern Optics **47**(14/15), 2000, pp. 2921–2931.
- [4] BERG-SØRENSEN K., FLYVBJERG H., *Power spectrum analysis for optical tweezers*, Review of Scientific Instruments **75**(3), 2004, pp. 594–612.
- [5] SIMMONS R.M., FINER J.T., CHU S., SPUDICH J.A., *Quantitative measurements of force and displacement using an optical trap*, Biophysical Journal **70**(4), 1996, pp. 1813–1822.
- [6] GRIER D.G., ROICHMAN Y., *Holographic optical trapping*, Applied Optics **45**(5), 2006, pp. 880–887.
- [7] COJOC D., GARBIN V., FERRARI E., BUSINARO L., ROMANATO F., DI FABRIZIO E., *Laser trapping and micro-manipulation using optical vortices*, Microelectronic Engineering **78–79**, 2005, pp. 125–131.
- [8] MCGLOIN D., DHOLAKIA K., *Bessel beams: diffraction in a new light*, Contemporary Physics **46**(1), 2005, pp. 15–28.
- [9] VAN DER HORST A., FORDE N.R., *Power spectral analysis for optical trap stiffness calibration from high-speed camera position detection with limited bandwidth*, Optics Express **18**(8), 2010, pp. 7670–7677.
- [10] CHERNOV N., *Fitting circles to scattered data: parameter estimates have no moments*, Metrika **73**(3), 2011, pp. 373–384.
- [11] GIBSON G.M., LEACH J., KEEN S., WRIGHT A.J., PADGETT M.J., *Measuring the accuracy of particle position and force in optical tweezers using high-speed video microscopy*, Optics Express **16**(19), 2008, pp. 14561–14570.

Received October 16, 2013